The Slp4-a linker domain controls exocytosis through interaction with Munc18-1・syntaxin-1a complex

doi: 10.1091/mbc.E05-11-1047

Molecular Biology of the Cell
Vol. 17, 2101–2112, May 2006

The Slp4-a Linker Domain Controls Exocytosis through Interaction with Munc18-1·Syntaxin-1a Complex[D]

Takashi Tsuboi* and Mitsunori Fukuda*†

*Fukuda Initiative Research Unit, Riken (The Institute of Physical and Chemical Research), Wako, Saitama 351-0198, Japan; and †Department of Developmental Biology and Neurosciences, Graduate School of Life Sciences, Tohoku University, Aoba-ku, Sendai, Miyagi 980-8578, Japan

Submitted November 15, 2005; Revised February 6, 2006; Accepted February 8, 2006
Monitoring Editor: Adam Linstedt

Synaptotagmin-like protein 4-a (Slp4-a)/granuphilin-a is specifically localized on dense-core vesicles in certain neuroendocrine cells and negatively controls dense-core vesicle exocytosis through specific interaction with Rab27A. However, the precise molecular mechanism of its inhibitory effect on exocytosis has never been elucidated and is still a matter of controversy. Here we show by deletion and chimeric analyses that the linker domain of Slp4-a interacts with the Munc18-1·syntaxin-1a complex by directly binding to Munc18-1 and that this interaction promotes docking of dense-core vesicles to the plasma membrane in PC12 cells. Despite increasing the number of plasma membrane docked vesicles, expression of Slp4-a strongly inhibited high-KCl–induced dense-core vesicle exocytosis. The inhibitory effect by Slp4-a is absolutely dependent on the linker domain of Slp4-a, because substitution of the linker domain of Slp4-a by that of Slp5 (the closest isoform of Slp4-a that cannot bind the Munc18-1·syntaxin-1a complex) completely abrogated the inhibitory effect. Our findings reveal a novel docking machinery for dense-core vesicle exocytosis: Slp4-a simultaneously interacts with Rab27A and Munc18-1 on the dense-core vesicle and with syntaxin-1a in the plasma membrane.

INTRODUCTION

Peptide hormones are stored in large dense-core vesicles in neuroendocrine cells and are released by exocytosis. Soluble *N*-ethylmaleimide-sensitive factor attachment protein receptors (SNAREs; Rothman, 1994; Jahn and Südhof, 1999; Rizo and Südhof, 2002) and Rab GTPases (Segev, 2001; Zerial and McBride, 2001) are thought to be required for biogenesis and trafficking of hormone-containing vesicles. The dense-core vesicle trafficking to the plasma membrane consists of at least three distinct steps: the transport of dense-core vesicles to the plasma membrane (recruitment), their initial interaction with the plasma membrane (docking or tethering), and their subsequent fusion with the plasma membrane (fusion). Although SNARE proteins are thought to regulate the final fusion step(s) in neuroendocrine cells (An and Almers, 2004), the molecular machinery involved in the initial docking or tethering step(s) remains largely unknown.

This article was published online ahead of print in *MBC in Press* (http://www.molbiolcell.org/cgi/doi/10.1091/mbc.E05–11–1047) on February 15, 2006.

[D] The online version of this article contains supplemental material at *MBC Online* (http://www.molbiolcell.org).

Address correspondence to: Mitsunori Fukuda (mnfukuda@brain.riken.go.jp).

Abbreviations used: GFP, green fluorescent protein; HA, hemagglutinin; HRP, horseradish peroxidase; mRFP, monomeric red fluorescent protein; NPY, neuropeptide Y; SHD, Slp homology domain; siRNA, small interfering RNA; Slac2, Slp homologue lacking C2 domains; Slp, synaptotagmin-like protein; SNAP-25, synaptosome-associated protein of 25 kDa; SNARE, soluble *N*-ethylmaleimide–sensitive factor attachment protein receptor; VAMP-2; vesicle-associated membrane protein-2; Venus, pH-insensitive yellow fluorescent protein; TIRF, total internal reflection fluorescence.

The synaptotagmin-like protein (Slp) family is a group of putative membrane trafficking proteins (Fukuda and Mikoshiba, 2001; Fukuda *et al.*, 2001) that are characterized by the presence of an N-terminal Slp homology domain (SHD), which functions as a Rab27-binding domain (Kuroda *et al.*, 2002a; Strom *et al.*, 2002; Yi *et al.*, 2002), and C-terminal tandem C2 domains (known as the C2A domain and C2B domain), putative Ca^{2+}-binding motifs (Fukuda, 2002). To date, five members of the Slp family (Slp1/Jfc1, Slp2-a, Slp3-a, Slp4-a/granuphilin-a, and Slp5) have been identified in the mouse and human (Wang *et al.*, 1999; Fukuda *et al.*, 2001; McAdara Berkowitz *et al.*, 2001; Kuroda *et al.*, 2002b). It has recently been proposed that members of the Slp family and of the Slp homologue lacking C2 domains (Slac2) family function as effector molecules for small GTPase Rab27A/B and regulate Rab27A/B-dependent secretion events (reviewed in Cheviet *et al.*, 2004; Fukuda, 2005). For example, Slp4-a/granuphilin-a is coexpressed with Rab27A in certain neuroendocrine cells, and both proteins are concentrated on dense-core vesicles (Wang *et al.*, 1999; Coppola *et al.*, 2002; Fukuda *et al.*, 2002; Yi *et al.*, 2002; Waselle *et al.*, 2003; Desnos *et al.*, 2003). Expression of Rab27A in pancreatic β-cell lines enhances depolarization-induced insulin secretion (Yi *et al.*, 2002), whereas expression of Slp4-a inhibits exocytosis in pancreatic β-cell lines, AtT20 cells, and PC12 cells (Fukuda *et al.*, 2002; Coppola *et al.*, 2002; Torii *et al.*, 2002; Zhao *et al.*, 2002), whereas other members of the Slp family are not inhibitory and instead promote dense-core vesicle exocytosis in PC12 cells (Fukuda *et al.*, 2002; Fukuda, 2003). However, the precise mechanism of the inhibitory effect by Slp4-a has never been elucidated and is still a matter of controversy (Coppola *et al.*, 2002; Fukuda, 2003; Torii *et al.*, 2004).

In this study we investigated the function of Slp4-a in the motion of a single dense-core vesicle during exocytosis by total internal reflection fluorescence (TIRF; also called evanescent

wave or evanescence) microscopy (Axelrod, 1981) with vesicle-targeted fluorescent proteins (Tsuboi *et al.*, 2000, 2003, 2004, 2005; Tsuboi and Rutter, 2003; Tsuboi and Fukuda, 2005). Expression of Slp4-a in PC12 cells induced a significant increase in the number of vesicles docked to the plasma membrane and a significant decrease in the number of single exocytotic events, without affecting release kinetics of peptide hormones. By contrast, RNA interference–mediated knockdown of endogenous Slp4-a resulted in a decrease in the number of docked vesicles and increase in the number of exocytotic events. Analysis using deletion mutants and chimeric Slp4-a proteins further indicated that the inhibitory effect of Slp4-a on exocytosis is dependent on its ability to bind Munc18-1, a SNARE-associated protein that binds the closed conformation of syntaxin-1a (Rizo and Südhof, 2002; Toonen and Verhage, 2003), and Rab27A. Based on these findings, we propose that Slp4-a is the fundamental machinery for anchoring dense-core vesicles to the plasma membrane through specific interaction with the Munc18-1·syntaxin-1a complex in neuroendocrine cells.

MATERIALS AND METHODS

Plasmid Construction

The following pairs of nucleotides with a 19-base target site (in bold) and a 9-base loop (underlined) were used to generate small interfering RNA (siRNA) expression plasmids against rat and mouse Slp4-a mRNA: Slp4-a siRNA(+) primer (5′-**AACTCCTGTGATGAAGAAG**TTCAAGAGACTTCTTCATCACAGGAGTTTTTTTT-3′) and Slp4-a siRNA(-) primer (5′-AATTAAAAAAA**AACTCCTGTGATGAAGAAG**TCTCTTGAACTTCTTCATCACAGGAGTTGGCC-3′). The pairs of nucleotides were mixed, denatured at 94°C for 2 min, annealed at 72°C for 1 min, gradually cooled to 4°C for 2 h, and then subcloned into the ApaI and EcoRI sites of the pSilencer 1.0-U6 vector (Ambion, Austin, TX), which expresses short hairpin RNA under the control of the mouse U6 promoter. The plasmid obtained was referred to as pSilencer-Slp4-a. The knockdown efficiency of pSilencer-Slp4-a was evaluated in COS7 cells or PC12 cells as described previously (Fukuda, 2004; Kuroda and Fukuda, 2004).

The Slp1, Slp2-a, Slp3-a, Slp4-a, Slp5, Slp3-a-ΔC2B, Slp3-a-ΔC2AB, Slp4-a-ΔC2B, Slp4-a-ΔC2AB, Slp5-ΔC2B, and Slp5-ΔC2AB cDNA fragments (Kuroda *et al.*, 2002a, 2002b; Fukuda *et al.*, 2005) were subcloned into the BamHI/NotI site of the pmRFP-C1-gk vector (Tsuboi and Fukuda, 2005) modified from pmRFP-C1 (BD Clontech, Palo Alto, CA) by introducing a short Gly linker just downstream of mRFP (monomeric red fluorescent protein; Campbell *et al.*, 2002). Plasmid encoding neuropeptide Y-tagged pH-insensitive yellow fluorescent protein, NPY-Venus (pVenus-N1-NPY), was generously provided by Dr. Atsushi Miyawaki (Nagai *et al.*, 2002). Other expression constructs were prepared as described elsewhere (see Fukuda *et al.*, 2005 and references therein).

Construction of Chimeric Plasmid between Slp4 and Slp5

The N-terminal SHD-swapping chimeras (Slp455 and Slp544; see Figure 5A) and the C2A-domain-swapping chimeras (Slp445 and Slp554) were prepared by two-step or conventional PCR techniques essentially as described previously (Fukuda *et al.*, 1995). For example, the Slp445 (i.e., Slp4-SHD+Slp4-linker+Slp5-C2A) cDNA was constructed by linking two separate PCR products: the Slp4-SHD+Slp4-linker fragment, amplified with the BOS-5′ primer (5′-GTTCATTCTCAAGCCTC-3′) and Slp4-linker-3′ primer (5′-AGATCTCACCGGTGACTTTCACGTTCCCAAAATCACCAGCTTCGCT-3′; BglII site, underlined) by using pEF-T7-Slp4-b as the template, and the Slp5-C2A fragment, amplified with the Slp5-C2A-5′ primer (5′-AGATCTTACTCCACATCAGCTAC-3′; BglII site, underlined) and BOS-3′ primer (5′-CACGTGGGAGACCTGAT-3′) by using pEF-T7-Slp5-ΔC2B as the template. These PCR products were subcloned into pGEM-T Easy vector (Promega, Madison, WI) and verified by DNA sequencing. The Slp5-C2A fragment was cleaved with BglII/SpeI and subcloned into the BglII/SpeI site of the pGEM-T-Slp4-SHD+linker. The pGEM-T-Slp445 obtained was cleaved with BamHI/NotI and subcloned into the BamHI/NotI site of the pmRFP-C1-gk vector (referred to as pmRFP-C1-Slp445). pmRFP-C1-Slp455, pmRFP-C1-Slp554, and pmRFP-C1-Slp544 were similarly constructed by using the above PCR techniques and the following primers: 5′-CCCGGGACTTCTCTTCTGGCGCAGGGACATCCT-3′ (Slp4-SHD-3′ primer; SmaI site, underlined) and 5′-CCCGGGTCTGAAGAAACACAAAACCAA-3′ (Slp5-linker-5′ primer; SmaI site, underlined); 5′-CTTAAGTGAAAAGGCAATCTTGCCCGTCACAGAGATGTTGCCATAGTCTCCCGTTTCACT-3′ (Slp5-linker-3′ primer; AflII site, underlined) and 5′-CTTAAGTTTGAGCAGAAAACACAG-3′ (Slp4-C2A-5′ primer; AflII site, underlined); and 5′-CTTAAGACCTGCAGTGAATAAAAGAGAG-3′ (Slp4-linker-5′ primer; AflII site, underlined). The linker domain-swapping chimeras (Slp454 and Slp545) were then produced by substitution of the BamHI/BstXI insert of pmRFP-C1-Slp455 for that of pmRFP-C1-Slp544 and by substitution of the BamHI/BstXI site of pmRFP-C1-Slp544 for that of pmRFP-C1-Slp445. The sequence of all plasmid inserts was verified by automated sequencing. The addition of the T7 tag to the N terminus of Slp445, Slp455, Slp554, Slp544, Slp454, and Slp545 and construction of expression vectors (pEF-T7-Slp445, pEF-T7-Slp455, pEF-T7-Slp554, pEF-T7-Slp544, pEF-T7-Slp454, and pEF-T7-Slp545) were performed as described previously (Mizushima and Nagata, 1990; Fukuda *et al.*, 1994, 1999).

Immunoprecipitation and Immunoblotting

COS-7 cells were cultured in DMEM supplemented with 10% fetal bovine serum (FBS), 100 U/ml penicillin G, and 100 μg/ml streptomycin. pEF-FLAG-syntaxin-1a, pEF-FLAG-Munc18-1, pEF-HA-Rab27A, or pEF-T7-Slp4/5 chimeric constructs (4 μg of plasmids in total) were transfected into COS7 cells (one confluent 10-cm dish) by using LipofectAmine Plus reagent according to the manufacturer's instructions. Cells were harvested 72 h after transfection and homogenized in 1 ml of the homogenization buffer as described previously (Fukuda and Kanno, 2005). The associations between these proteins were evaluated by immunoprecipitation as described previously (Fukuda, 2003; Fukuda and Kanno, 2005). Immunoreactive bands were visualized with horseradish peroxidase (HRP)-conjugated anti-T7 tag antibody (1/10,000; Novagen, Madison, WI), HRP-conjugated anti-FLAG tag antibody (M2; 1/10,000 dilution; Sigma Chemical Co., St. Louis, MO), and HRP-conjugated anti-HA tag antibody (1/10,000; Sigma Chemical Co.), and detected by enhanced chemiluminescence (ECL; Amersham Biosciences, Buckinghamshire, United Kingdom).

PC12 cells were cultured in DMEM supplemented with 10% FBS, 10% horse serum, 100 U/ml penicillin G, and 100 μg/ml streptomycin, at 37°C under 5% CO_2. pEF-T7-Slp4-b, pEF-T7-Slp454, pEF-T7-Slp5-ΔC2B, or pEF-T7-Slp545 chimeric plasmids (4 μg of plasmids in total) were transfected into PC12 cells (2×10^6 cells, the day before transfection/10-cm dish) by using LipofectAmine 2000 according to the manufacturer's instructions. Cells were harvested 72 h after transfection and homogenized in 1 ml of a buffer containing 50 mM HEPES-KOH, pH 7.2, 250 mM NaCl, 0.5 mM GTPγS, 0.1 mM phenylmethylsulfonyl fluoride, 10 μM leupeptin, and 10 μM pepstatin A. After solubilization with 1% Triton X-100 at 4°C for 1 h, the supernatants (400 μl) were obtained by centrifugation at 15,000 rpm for 10 min. After incubation with anti-T7 tag antibody-conjugated agarose (wet volume 15 μl; Novagen) at 4°C for 1 h, the beads were washed five times with 1 ml of 50 mM HEPES-KOH, pH 7.2, 250 mM NaCl, 0.2% Triton X-100, and protease inhibitors and then resuspended in SDS sample buffer. Immunoprecipitates were subjected to 10% SDS-PAGE followed by immunoblotting with anti-syntaxin-1 antibody (1/100 dilution; Santa Cruz Biotechnology, Santa Cruz, CA), anti-Munc18-1 antibody (1/100 dilution; BD Transduction Laboratories, Lexington, KY), and anti-Rab27A antibody (2 μg/ml; Imai *et al.*, 2004). Immunoreactive bands were visualized with HRP-conjugated goat anti-mouse or anti-rabbit IgG (1/10,000 dilution) and detected by ECL. Expression of actin, SNAP-25 (synaptosome-associated protein of 25 kDa), and VAMP-2 (vesicle-associated membrane protein-2) in PC12 cells was investigated by immunoblotting with commercially available antibodies as described previously (Fukuda, 2004).

Confocal Imaging

For microscopic analysis, PC12 cells were fixed with 4% paraformaldehyde (Wako Pure Chemicals, Osaka, Japan) for 20 min. For immunostaining, cells were permeabilized with 0.3% Triton X-100 for 2 min and blocked with the blocking buffer (1% BSA and 0.1% Triton X-100 in PBS) for 1 h. The cells were then immunostained with the primary antibodies, followed by Alexa-Fluor 488–labeled or 568–labeled secondary IgG (1/5000 dilution; Molecular Probes, Eugene, OR). The cells were examined for fluorescence with a confocal laser-scanning microscope (Fluoview 500, Olympus, Tokyo, Japan), and the images were processed with MetaMorph software (version 6.3, Universal Imaging, Downingtown, PA).

TIRF Microscopy

PC12 cells were cultured as described above. For TIRF imaging, PC12 cells were plated onto poly-L-lysine–coated coverslips and then cotransfected with 1 μg of pVenus-N1-NPY, and either 3 μg of pmRFP-C1 (a vector control), pmRFP-C1-Slp1~5, or pmRFP-C1–4/5-swapping constructs by using LipofectAmine 2000 reagent according to the manufacturer's instructions. To knockdown endogenous Slp4-a protein expression, we cotransfected with 3 μg of pSilencer-Slp4-a vector and 1 μg of NPY-Venus vector into PC12 cells. Expression of each mRFP fusion protein and NPY-Venus was confirmed by immunoblotting with anti-DsRed antibody (1/250 dilution; MBL, Nagoya, Japan) and anti-GFP (green fluorescent protein) antibody (1/250 dilution; MBL), respectively. Expression of mRFP-Slp and endogenous Slp proteins in PC12 cells was also investigated by immunoblotting with isoform-specific antibodies as described previously (Imai *et al.*, 2004; Supplementary Figure 1). Based on the relative signals of exogenous mRFP-Slp4-a and endogenous Slp4-a (mRFP-Slp4-a/endogenous Slp4-a, 9.1:1) and the maximum transfection efficiency (~50%), the expression levels of transiently expressed Slp4-a (or presumably other Slps and their mutants) were estimated to be ~18 times higher than those of endogenous Slp4-a (Supplementary Figure 1D). The

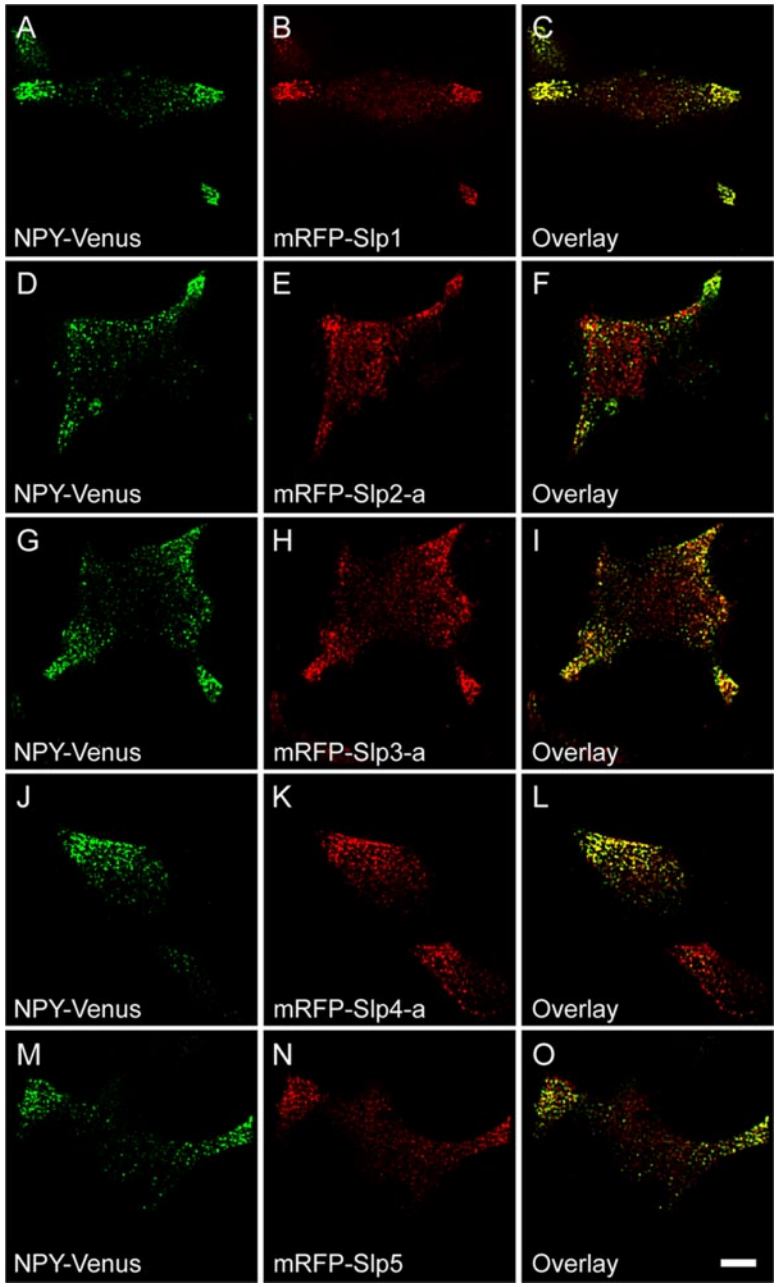

Figure 1. Colocalization of Slp proteins with secretory vesicles in PC12 cells. NPY-Venus (A, D, G, J, and M) and mRFP-Slp1 (B), mRFP-Slp2-a (E), mRFP-Slp3-a (H), mRFP-Slp4-a (K), or mRFP-Slp5 (N) were coexpressed in PC12 cells, and images of the fixed cells were obtained by confocal microscopy. Note that all five mRFP-Slps colocalized well with NPY-Venus, a dense-core vesicle marker (C, F, I, L, and O). Scale bar, 5 μm.

imaging was performed at 37°C in a modified Ringer buffer (RB: 130 mM NaCl, 3 mM KCl, 5 mM $CaCl_2$, 1.5 mM $MgCl_2$, 10 mM glucose, and 10 mM HEPES, pH 7.4). Stimulation with high-KCl was achieved by perfusion with 70 mM KCl containing RB (NaCl was reduced to maintain the osmolarity). Exocytosis of NPY-Venus at the single vesicle level was monitored with a TIRF microscope essentially as described previously (Tsuboi *et al.*, 2000, 2003, 2004, 2005; Tsuboi and Rutter, 2003; Tsuboi and Fukuda, 2005). Images were acquired every 200 ms, or otherwise as indicated. To analyze the TIRF imaging data, single exocytotic events were selected manually (see below for details), and the average fluorescence intensity of individual vesicle in a 0.7 × 0.7-μm square placed over the vesicle center was calculated. To distinguish between fusion events and vesicle movement (i.e., vesicles pause at the plasma membrane and then move back inside the cell without fusing), we focused on fluorescence changes just before the disappearance of fluorescent signals. When there was a fusion event, a rapid transient increase in fluorescence intensity (to a peak intensity 1.5 times greater than the original fluorescence intensity within 1 s) was observed, whereas when vesicles moved, the fluorescence intensity gradually decreased to the background level (see closed squares and open circles, respectively, in Figure 3B). The number of fusion events during a 5-min period was counted manually based on the above criteria. Data are reported as means ± SE of at least five individual experiments. Means were compared by one-way ANOVA with GraphPad Prism software (GraphPad Software, San Diego, CA).

RESULTS

Slp Family Proteins Are Associated with Dense-Core Vesicles in PC12 Cells

To determine whether Slp family members are specifically targeted to dense-core vesicles, we simultaneously labeled the dense-core vesicle cargo and Slp family proteins in PC12 cells by coexpressing pH-insensitive yellow fluorescent protein mutant-tagged neuropeptide Y (NPY-Venus), which are efficiently targeted to the dense-core vesicles (Nagai *et al.*, 2002), and monomeric red fluorescent protein (mRFP)-tagged Slp1~5. Confocal microscopy revealed that most NPY-Venus–positive

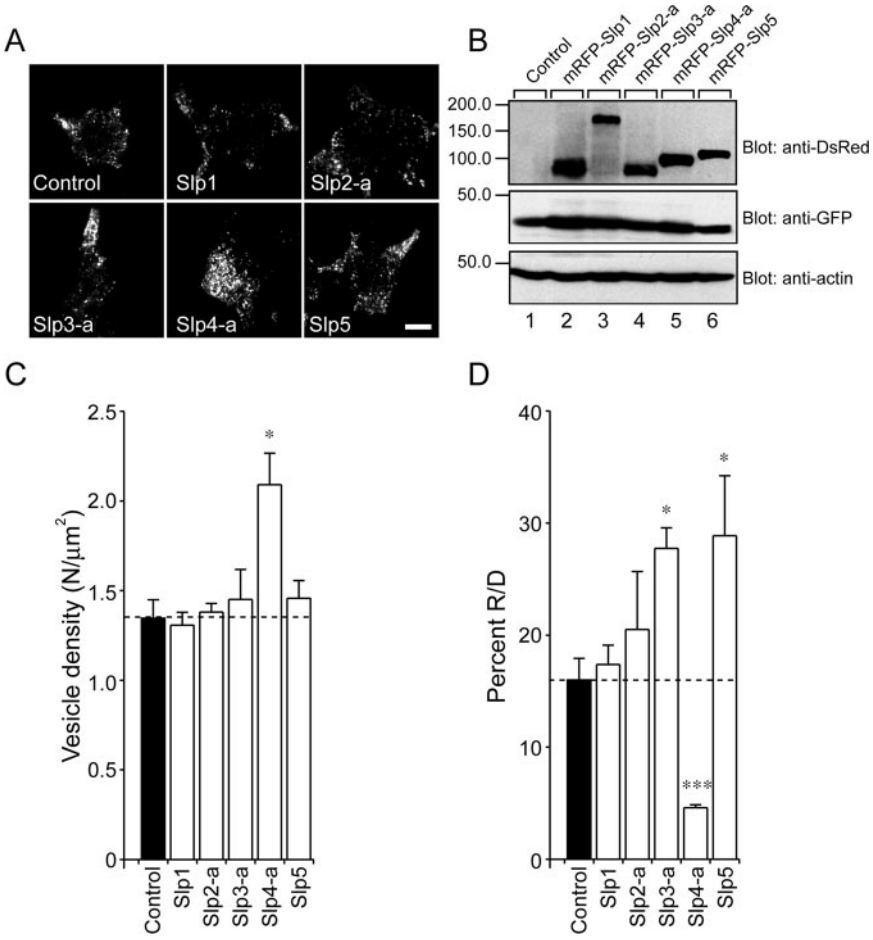

Figure 2. Effect of expression of Slp1~5 on the number of vesicles docked to the plasma membrane of PC12 cells. (A) Typical TIRF images of plasma membrane-docked NPY-Venus vesicles observed before high-KCl stimulation in control (control), mRFP-Slp1–expressing (Slp1), mRFP-Slp2-a–expressing (Slp2-a), mRFP-Slp3-a–expressing (Slp3-a), mRFP-Slp4-a–expressing (Slp4-a), and mRFP-Slp5–expressing cells (Slp5). Scale bar, 5 μm. (B) Expression of mRFP-Slp1~5, NPY-Venus, and actin in PC12 cells was analyzed by 10% SDS-PAGE followed by immunoblotting with anti-DsRed antibody (1/250 dilution), anti-GFP antibody (1/250 dilution), and anti-actin (1/300 dilution) antibody, respectively. The positions of the molecular mass markers ($\times 10^{-3}$) are shown on the left. (C) The density of docked vesicles was determined by counting the vesicles in each image (n = 6 cells in each). (D) The percent of the number of NPY-Venus release events (R) during the 5-min stimulation to the number of plasma membrane-docked vesicles (D) before stimulation in mRFP-Slp–expressing cells obtained by TIRF microscopy (n = 6 cells in each). Data are shown as mean values ± SE. *,*** $p < 0.05$ and 0.001, respectively, in comparison with the control. Note that expression of mRFP-Slp4-a significantly increased the number of plasma membrane–docked vesicles (C) and decreased the percent R/D values (D).

vesicles colocalized with mRFP-Slp1–positive vesicles (Figure 1, A–C; 83.5 ± 4.6%, 7 cells), indicating efficient targeting of mRFP-Slp1 to dense-core vesicles, where Rab27A is enriched. Similarly, most mRFP-Slp2-a- (Figure 1, D–F; 73.4 ± 5.6%, 6 cells), mRFP-Slp3-a- (Figure 1, G–I; 91.1 ± 6.6%, 5 cells), mRFP-Slp4-a- (Figure 1, J–L; 87.4 ± 7.3%, 6 cells), and mRFP-Slp5-labeled (Figure 1, M–O; 73.2 ± 3.2%, 5 cells) structures colocalized with NPY-Venus.

Slp4-a, But Not Other Slps, Increased the Number of Vesicles Docked to the Plasma Membrane and Inhibited the Number of Exocytotic Events

The efficient targeting of mRFP-Slp proteins to dense-core vesicles that contain NPY-Venus has enabled us to further analyze the impact of Slp proteins on the dynamics of single exocytotic events within ~100 nm beneath the plasma membrane in PC12 cells by TIRF microscopy (Tsuboi and Fukuda, 2005). Counting the number of plasma membrane-docked vesicles in resting PC12 cells by TIRF microscopy revealed that expression of mRFP-Slp4-a significantly increased (to 155.9%) the number of plasma membrane-docked vesicles (Figure 2, A, bottom middle panel, and C), whereas expression of other Slps had no effect at all. The effect by Slp4-a should not be attributable to the change in the total number of vesicles or the excess amount of mRFP-Slp4-a protein, because the expression levels of NPY-Venus in the control and mRFP-Slp–expressing cells were almost similar (Figure 2B, middle panel) and the same expression levels of mRFP-Slp1~5 were observed (Figure 2B, top panel). Next we counted the total number of NPY-Venus release events (i.e., dense-core vesicle exocytosis) by cells expressing NPY-Venus together with each mRFP-Slp member during high-KCl (70 mM) stimulation. Because the number of plasma membrane–docked vesicles before stimulation and number of NPY-Venus release events differed between the transfected cells, we measured the number of NPY-Venus release events (R) during the 5-min stimulation period and the number of plasma membrane-docked vesicles (D) before stimulation and then calculated the ratio between R and D (R/D expressed as a percent; i.e., normalized NPY-Venus release events). Despite increasing the number of vesicles docked to the plasma membrane, the number of NPY-Venus release events in the mRFP-Slp4-a–expressing cells was reduced, and the percent R/D value was thus reduced to 28.7% in comparison with the control. By contrast, expression of mRFP-Slp3-a and mRFP-Slp5 significantly increased the percent R/D values to 173.4 and 180.5%, respectively, and mRFP-Slp1 and mRFP-Slp2-a were again neutral in terms of normalized NPY-Venus release events (Figure 2D), consistent with the previous biochemical analyses (Fukuda *et al.*, 2002; Fukuda, 2003; Torii *et al.*, 2002).

Effect of Expression of Slp3-a, Slp4-a, or Slp5 on the Kinetics of Vesicle Fusion

To further determine whether the expression of mRFP-Slp3-a, -Slp4-a, or -Slp5 modulates the kinetics of vesicle exocytosis, the dynamics of single vesicle fusion events in a single NPY-Venus–expressing vesicle near the plasma membrane was analyzed by TIRF microscopy. High-KCl stimulation of Ca^{2+} influx caused

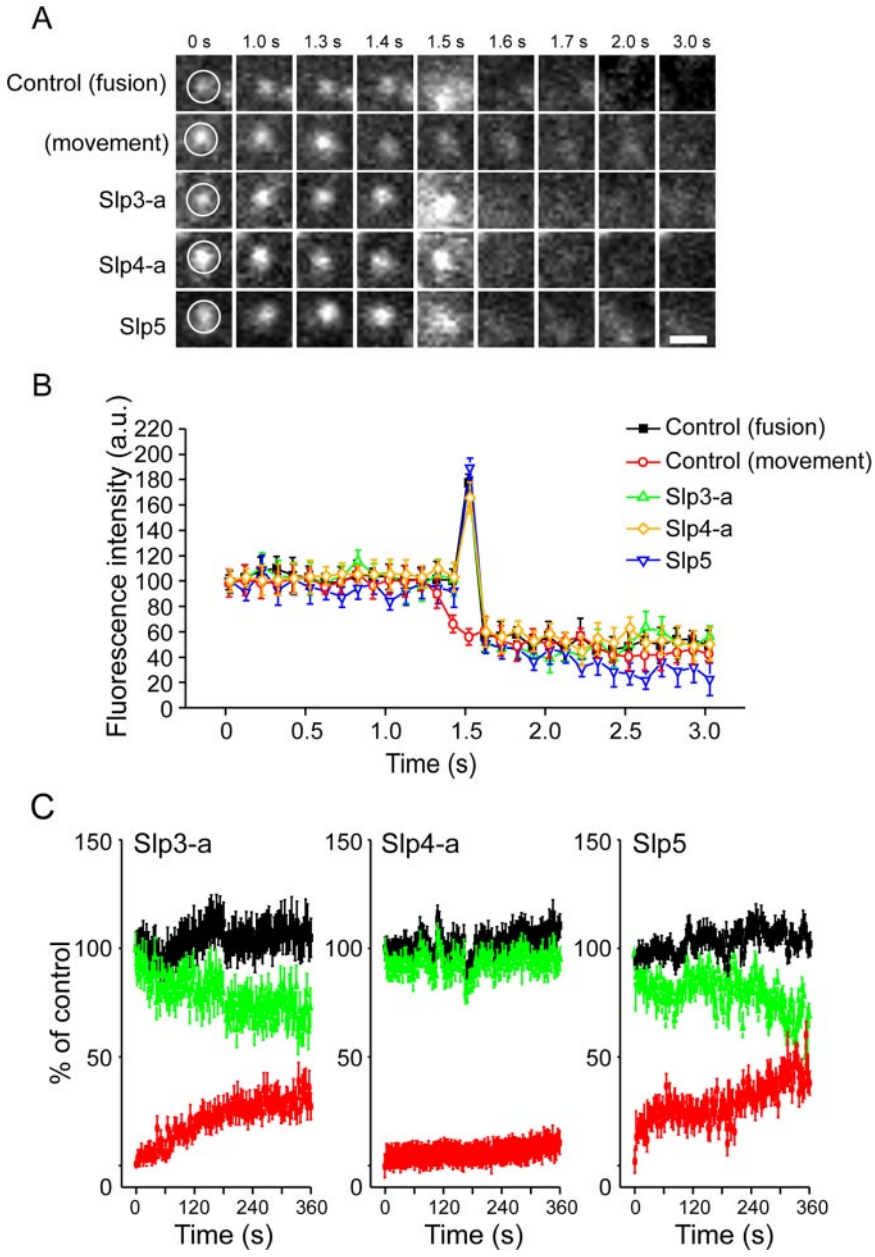

Figure 3. Effect of mRFP-Slp3-a, mRFP-Slp4-a, and mRFP-Slp5 expression on the kinetics of NPY-Venus release. (A) Typical sequential images acquired under the TIRF microscope at 100-ms intervals of a single NPY-Venus vesicle observed after high-KCl (70 mM) stimulation in cells coexpressing a control vector (control (fusion)), mRFP-Slp3-a (Slp3-a), mRFP-Slp4-a (Slp4-a), or mRFP-Slp5 (Slp5). The fifth images (1.5 s) show a diffuse cloud of NPY-Venus fluorescence, and the sixth images (1.6 s) show disappearance of the spot. By contrast, no diffuse cloud of NPY-Venus fluorescence was observed in the control (movement) vesicle (1.5 s) and then the vesicle was gradually disappeared from the evanescent field (1.6–3.0 s). (B) Time course of the fluorescence changes measured in the center of NPY-Venus vesicles in control (fusion; ■), control (movement; ○), mRFP-Slp3-a–expressing (Δ), mRFP-Slp4-a–expressing (◇), and mRFP-Slp5–expressing (▽) cells. The average fluorescence intensity before fusion was set equal to 100% (n = 15 vesicles in each). Images were acquired every 100 ms in each condition. Note that overexpression of Slp3-a, Slp4-a, or Slp5 had no effect on the release kinetics of NPY-Venus by the dense-core vesicles. By contrast, no spike increase in the fluorescence intensity was observed in the control (movement) vesicle. (C) Time-dependent change of the number of NPY-Venus vesicles docked to the plasma membrane during high-KCl stimulation. The number of previously docked vesicles that do not undergo exocytosis (green lines) and the number of newly recruited docked vesicles that either dock or undergo exocytosis (red lines) during the stimulation were determined by counting vesicles on each image (30–50 vesicles in 25-μm^2 area, n = 5 cells in each) in mRFP-Slp3-a– (left), mRFP-Slp4-a– (middle), and mRFP-Slp5–expressing cells (right). The black line shows the total number of docked vesicles, corresponding to the sum of the green and red lines. Time 0 indicates the addition of the stimulation. The number of previously docked vesicles at time 0 was taken as 100%. Data are shown as mean values ± SE.

NPY-Venus–containing spots to suddenly brighten and spread (Figure 3, A, control (fusion) panels, and B, closed squares), consistent with release of the fluorescent peptides (Lang *et al.*, 1997; Tsuboi *et al.*, 2003, 2004, 2005; Tsuboi and Rutter, 2003; Tsuboi and Fukuda, 2005). By contrast, no diffuse cloud of NPY-Venus fluorescence was observed in nonsecretory events (see Figure 3, A, control (movement) panels, and B, open circles). Although exocytotic events were detected much less frequently in the mRFP-Slp4-a–expressing cells than in the control cells, or mRFP-Slp3-a- or mRFP-Slp5–expressing cells, the kinetics of individual NPY-Venus release events was identical in all cells (Figure 3B).

To clarify whether the accumulation of docked vesicles was secondary to a decrease in the fusion probability in mRFP-Slp4-a–expressing cells, we investigated the change in total number of vesicles docked to the plasma membrane during high-KCl stimulation by tracking the motion of each docked vesicle on sequential images. In mRFP-Slp3-a- or mRFP-Slp5–expressing cells, the number of previously docked vesicles (i.e., vesicles that had already docked to the plasma membrane before stimulation) gradually decreased as a result of fusion or vesicle retreat (vesicles paused at the plasma membrane and then moved back inside the cell without fusing; green lines in Slp3-a and Slp5 panels of Figure 3C), whereas the number of newly recruited docked vesicles rapidly and progressively increased after stimulation (red lines in Slp3-a and Slp5 panels of Figure 3C). As a result, the total number of docked vesicles (previously docked vesicles plus newly recruited docked vesicles) increased to ~110% of the initial number of docked vesicles (black lines in Slp3-a and Slp5 panels of Figure 3C). By contrast, the increase in the number of newly recruited docked vesicles in mRFP-Slp4-a–expressing cells was almost completely prevented (red line in Slp4-a panel of Figure 3C), and no change in the number of previously docked vesicles was observed (green line in Slp4-a panel of Figure 3C). These results indicate that Sp4-a increases the number of "inert vesicles" docked to the plasma membrane and decreases the number of newly re-

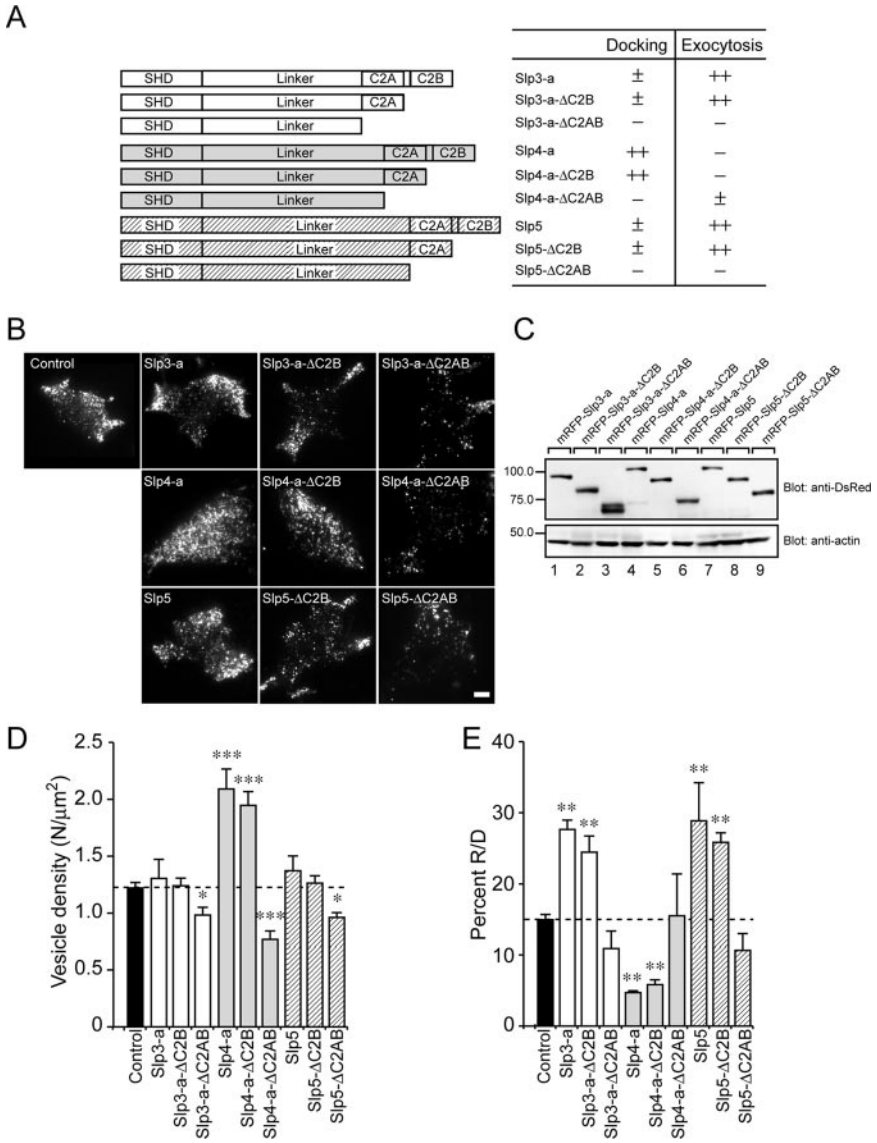

Figure 4. Effect of the deletion mutants of Slps on the number of vesicles docked to the plasma membrane of PC12 cells. (A) Schematic representation of the deletion mutants of Slp3-a, Slp4-a, and Slp5 (i.e., ΔC2B and ΔC2AB). The effects of each mutant on plasma membrane-docked vesicles and exocytosis (−, ±, ++) are indicated after its name. (B) Typical TIRF images of plasma membrane–docked vesicles observed before high-KCl stimulation in control (control), mRFP-Slp3-a–expressing (Slp3-a), mRFP-Slp3-a-ΔC2B–expressing (Slp3-a-ΔC2B), mRFP-Slp3-a-ΔC2AB–expressing (Slp3-a-ΔC2AB), mRFP-Slp4-a–expressing (Slp4-a), mRFP-Slp4-a-ΔC2B–expressing (Slp4-a-ΔC2B), mRFP-Slp4-a-ΔC2AB–expressing (Slp4-a-ΔC2AB), mRFP-Slp5–expressing (Slp5), mRFP-Slp5-ΔC2B–expressing (Slp5-ΔC2B), and mRFP-Slp5-ΔC2AB–expressing (Slp5-ΔC2AB) cells. Scale bar, 5 μm. (C) Expression of the deletion mutants of Slps and actin in PC12 cells visualized with anti-DsRed antibody and anti-actin antibody, respectively. The positions of the molecular mass markers ($\times 10^{-3}$) are shown on the left. (D) The density of docked vesicles was determined by counting the vesicles in each image (n = 6 cells in each). (E) The effect of expression of deletion mutants of Slps on the percent R/D values (n = 6 cells in each). Data are shown as mean values ± SE. *,**,*** $p < 0.05$, 0.01, and 0.001, respectively, in comparison with the control. Note that the expression of Slp mutants lacking the C2B domain (i.e., ΔC2B) had effects similar to those of the wild-type Slps with regard to the number of plasma membrane–docked vesicles (D) and the percent R/D values (E), whereas expression of Slp mutants lacking the C2AB domains (i.e., ΔC2AB) significantly decreased the number of plasma membrane–docked vesicles (D) without altering the percent R/D values (E).

cruited docked vesicles during the stimulation, presumably by occupying most of the plasma membrane docking sites. As a result, Slp4-a dramatically decreases NPY release events (i.e., decease in the percent R/D value). By contrast, Slp3-a and Slp5 increase the number of newly recruited docked vesicles, but not of previously docked vesicles, during the stimulation and increase NPY release events (i.e., increase in the percent R/D value).

The Linker Domain and the C2A Domain of Slp3-a, Slp4-a, and Slp5 are Essential to Modulation of Dense-Core Vesicle Exocytosis

In the next set of experiments we performed a systematic deletion analysis to identify the mechanism of regulation of dense-core vesicle exocytosis by Slp3-a, Slp4-a, or Slp5. Because we previously demonstrated that the SHD is required for targeting to Rab27A on dense-core vesicles (Fukuda, 2003), we predicted that the linker domain or two C2 domains are involved in the association with the plasma membrane and produced two types of truncated mutants (i.e., mRFP-Slp-ΔC2B and mRFP-Slp-ΔC2AB; summarized in Figure 4A). We first confirmed that the expression levels of these truncated mutants in PC12 cells were similar to those of the full-length proteins (Figure 4C) and then performed TIRF microscopic analysis as described above. Interestingly, expression of mRFP-Slp-ΔC2B had the same effects as expression of the full-length proteins did, indicating that the C2B domain of Slp3∼5 is not required for the control of dense-core vesicle exocytosis (Figure 4, D and E). By contrast, deletion of the two C2 domains (i.e., mRFP-Slp-ΔC2AB) completely abrogated the function of Slp3-a, Slp4-a, and Slp5 (Figure 4, D and E). The number of plasma membrane–docked vesicles in all three ΔC2AB mutants was significantly decreased, even compared with the control cells (Figure 4, B and D), and the ΔC2AB mutants had no or little effect on the percent R/D (i.e., normalized NPY-Venus release events; Figure 4E), indicating that the C2A domain, but not the C2B domain, are required for the control of dense-core vesicle exocytosis by Slp3-a, Slp4-a, and Slp5.

The Linker Domain of Slp4-a Mediates Vesicle Docking to the Plasma Membrane

To further determine which domains (SHD, linker, C2A domain) of Slp4-a primarily mediate the docking of dense-

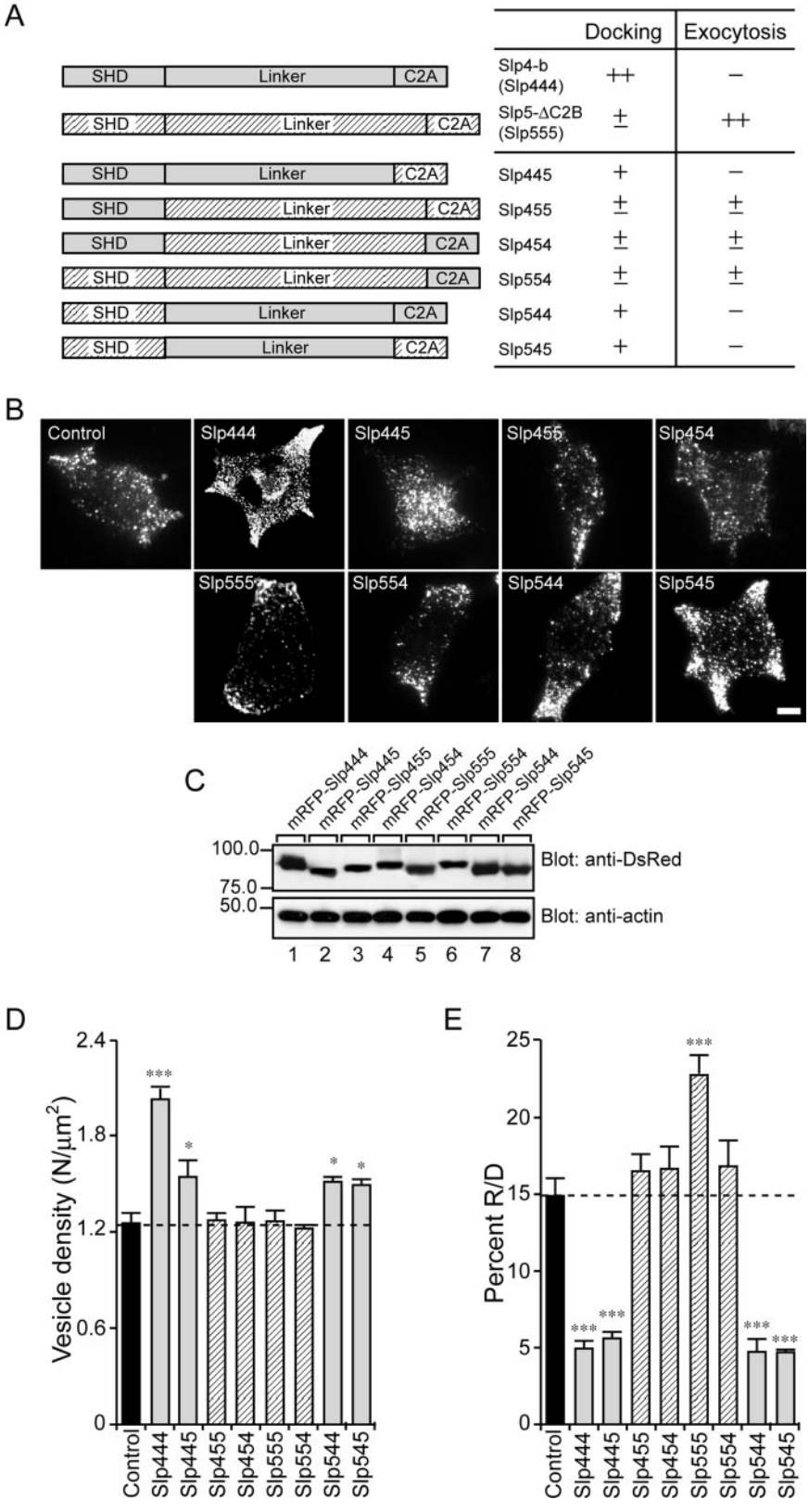

Figure 5. Effect of the Slp4/5 chimeras on the number of vesicles docked to the plasma membrane of PC12 cells. (A) Schematic representation of Slp4/5 chimeras. The effects of each mutant on plasma membrane–docked vesicles and exocytosis (−, ±, +, ++) are indicated after its name. (B) Typical TIRF images of plasma membrane–docked vesicles observed before high-KCl stimulation in control (control), mRFP-Slp444, mRFP-Slp445, mRFP-Slp455, mRFP-Slp454, mRFP-Slp555, mRFP-Slp554, mRFP-Slp544, and mRFP-Slp545 cells. Scale bar, 5 μm. (C) Expression of the Slp4/5 chimeras and actin in PC12 cells visualized with anti-DsRed antibody and anti-actin antibody, respectively. The positions of the molecular mass markers ($\times 10^{-3}$) are shown on the left. (D) The density of docked vesicles was determined by counting the vesicles in each image (n = 6 cells in each). (E) The effect of expression of the Slp4/5 chimeras on the percent R/D. Data are shown as mean values ± SE. *,*** $p < 0.05$, and 0.001, respectively, in comparison with the control. Note that the expression of Slp4-a-linker-domain–containing chimeras (i.e., Slp444, Slp445, Slp544, and Slp545; gray bars) significantly increased the number of plasma membrane-docked vesicles (D) but decreased the percent R/D values (E).

core vesicles to the plasma membrane, we prepared six different chimeric constructs between Slp4-a and Slp5 and assessed their plasma membrane–docking activity by TIRF microscopy (summarized in Figure 5A). The results clearly showed that the linker domain of Slp4-a is responsible for vesicle docking to the plasma membrane (Figure 5, B and D). Replacement of the linker domain of Slp4-a by the Slp5 linker (i.e., Slp4-SHD+Slp5-linker+Slp4-C2A; hereafter sim-

ply referred to as Slp454) completely abrogated the vesicle-docking activity. Similarly, both the Slp455 and Slp554 chimeras, which contain the linker domain of Slp5, failed to promote vesicle docking to the plasma membrane (hatched bars in Figure 5D). By contrast, the Slp445, Slp544, and Slp545 chimeras, which contain the linker domain of Slp4-a showed a significant increase in the number of plasma membrane–docked vesicles (gray bars in Figure 5D), although the vesicle-docking activity of these chimeras were weaker than that of Slp4-b (i.e., Slp444). Moreover, expression of the Slp4-a linker–containing chimeras (i.e., Slp445, Slp544, and Slp545 chimeras) significantly reduced the percent R/D values (normalized NPY-Venus release events), whereas other chimeras that contain the Slp5-linker domain had no significant effect (Figure 5E). These results cannot be explained by the different expression levels of chimeric constructs, because the expression levels of Slp4-b (i.e., Slp444), Slp5-ΔC2B (i.e., Slp555), and other chimeric constructs in PC12 cells were almost the same (Figure 5C). We therefore concluded that the linker domain of Slp4-a is responsible for the vesicle-docking to the plasma membrane as well as for the reduction of the percent R/D value, although the linker domain alone is not sufficient for such activities and adjacent SHD and C2A domains are also required.

The results of the chimeric analysis between Slp4 and Slp5 also provided important information about the promotion of NPY-Venus release by Slp5. Because the Slp455 and Slp554 chimeras did not significantly increase the percent R/D values, the Slp4-a SHD and the Slp4-a C2A domain cannot substitute for the function of the Slp5 SHD and the Slp5 C2A domain, respectively. Actually, the SHDs of Slp4-a and Slp5 have been shown to differ, because only the former SHD interacts with Rab27A(T23N), which mimics the GDP-bound form of Rab27A (Fukuda, 2003), and the C2A domains of Slp4-a and Slp5 have been shown to be different, because only the latter C2A domain exhibits Ca^{2+}-dependent phospholipid-binding activity (Wang *et al.*, 1999; Fukuda, 2002; Kuroda *et al.*, 2002b). These results suggest that both the GTP-dependent Rab27A-binding ability and the Ca^{2+}-dependent phospholipid-binding ability of Slp5 are necessary for it to exert its function during dense-core vesicle exocytosis.

Silencing of Slp4-a with siRNA Reduces the Number of Vesicles Docked to the Plasma Membrane and Increases the Number of Exocytotic Events

Because we showed that Slp4-a, but not other Slps, is endogenously expressed in PC12 cells (Fukuda *et al.*, 2002, and see Supplementary Figure 1), we explored the role of endogenous Slp4-a in dense-core vesicle exocytosis by RNA interference technology combined with TIRF microscopy. Expression of the Slp4-a siRNA reduced endogenous expression of Slp4-a (Figure 6A, top, lane 2) in PC12 cells, whereas a control pSilencer vector had no effect at all (Figure 6A, top, lane 1). In addition, expression of the Slp4-a siRNA had no effect on endogenous expression of other exocytotic proteins, including Munc18-1, syntaxin-1a, SNAP-25, VAMP-2, and Rab27A (Figure 6A). We therefore concluded that the Slp4-a siRNA specifically down-regulates endogenous Slp4-a in PC12 cells. Interestingly, expression of the Slp4-a siRNA (Figure 6, B and C) significantly reduced the number of plasma membrane–docked vesicles (to 60.1%), compared with the control cells (Figure 6, C and D), and, to our surprise, the percent of R/D value was increased to 180.4% in the Slp4-a-siRNA–expressing cells, compared with the control cells (Figure 6D).

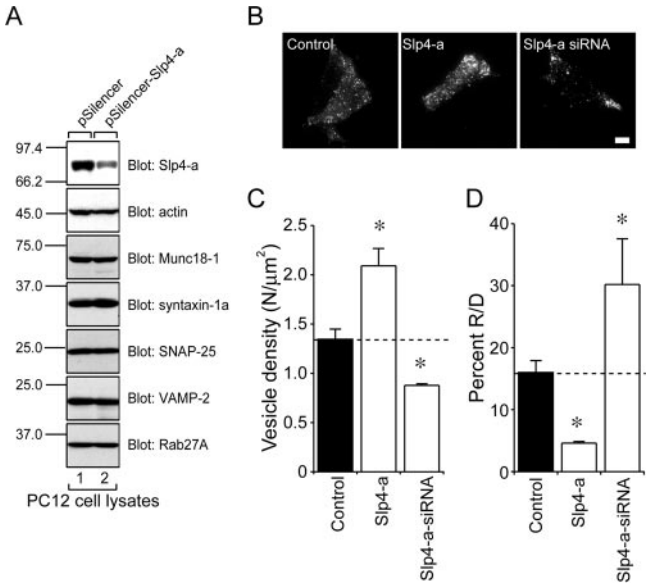

Figure 6. Effect of Slp4-a siRNA expression on the number of vesicles docked to the plasma membrane of PC12 cells. (A) Effect of Slp4-a siRNA on expression of Slp4-a in PC12 cells. PC12 cells were transfected with pSilencer-Slp4-a (lane 2) or a control vector (lane 1). Cell lysates were prepared and subjected to 12.5% SDS-PAGE followed by immunoblotting with anti-Slp4-a (Imai *et al.*, 2004), anti-actin (1/300 dilution), anti-Munc18-1 (1/100 dilution), anti-syntaxin-1a (1/100 dilution), anti-SNAP-25 (1/1000 dilution), anti-VAMP-2 (1/100 dilution), and anti-Rab27A antibody (3 μg/ml). The positions of the molecular mass markers ($\times 10^{-3}$) are shown on the left. (B) Typical TIRF images of plasma membrane–docked vesicles before high-KCl stimulation of control (left), Slp4-a–expressing (middle), and Slp4-a-siRNA–expressing cells (right). Scale bar, 5 μm. (C) The density of docked vesicles was determined by counting the vesicles in each image (n = 7 cells in each). (D) The effect of the Slp4-a siRNA on the percent R/D values (n = 7 cells in each). The data are mean values ± SE. * $p < 0.05$ in comparison with the control. Note that expression of the Slp4-a siRNA significantly reduced the number of plasma membrane–docked vesicles (C) and increased the percent R/D values (D).

The Linker Domain of Slp4-a Interacts with Munc18-1 in PC12 Cells

In the final set of experiments, we attempted to determine how the Slp4-a linker domain controls dense-core vesicle exocytosis at the molecular level. Because it has recently been shown that Slp4-a interacts with t-SNARE syntaxin-1a and/or Munc18-1 (Coppola *et al.*, 2002; Torii *et al.*, 2002, 2004; Fukuda, 2003; Fukuda *et al.*, 2005), we first investigated the interaction between Slp4/Slp5 chimeras and Munc18-1 and syntaxin-1a by coimmunoprecipitation assay in COS-7 cells, which do not endogenously express neuronal SNARE-related proteins (Fukuda *et al.*, 2005). In brief, agarose beads coupled with each T7-tagged Slp4/Slp5 chimera were incubated with FLAG-Munc18-1, FLAG-syntaxin-1a, and HA-Rab27A, and proteins trapped with the beads were analyzed by immunoblotting (Figure 7). It was very interesting to find that only the Slp4-linker-domain–containing chimeras (i.e., Slp445, Slp544, and Slp545) interacted with both Munc18-1 and syntaxin-1a (lanes 1, 2, 7, and 8 in Figure 7, A and B), although all chimeras interacted normally with Rab27A (Figure 7C). The interaction between Slp4 and syntaxin-1a must be indirect, because syntaxin-1a failed to interact with Sp4-a in the absence of Munc18-1 (Fukuda, 2003; but see

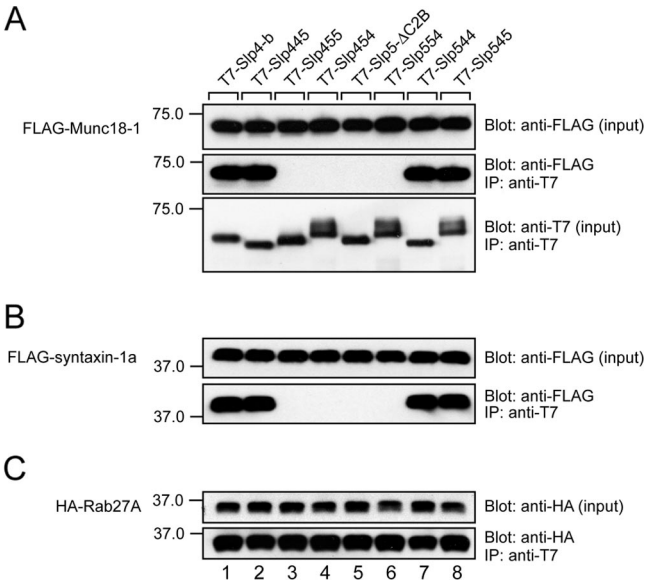

Figure 7. Munc18-1 and syntaxin-1a interact with Slp4-a in a Slp4-linker-domain–dependent manner. Beads coupled with each T7-Slp4/5 chimera were incubated with FLAG-Munc18-1, FLAG-syntaxin-1a, and HA-Rab27A, and coimmunoprecipitated FLAG-tagged proteins and HA-Rab27A were detected with HRP-conjugated anti-FLAG tag antibody (Blot: anti-FLAG, in A and B) and HRP-conjugated anti-HA tag antibody (Blot: anti-HA, in C), respectively. The same blots were then stripped and reprobed with HRP-conjugated anti-T7 tag antibody to ensure that equivalent amounts of T7-tagged proteins had been loaded (Blot: anti-T7, bottom panel in A). Input means one tenth the volume of the reaction mixture used for immunoprecipitation (IP). The positions of the molecular mass markers ($\times 10^{-3}$) are shown on the left. Note that Slp4-linker-domain-containing chimeras (i.e., Slp445, Slp544, or Slp545) interacted with both Munc18-1 and syntaxin-1a (lanes 1, 2, 7, and 8 in the middle panel of A and the bottom panel in B).

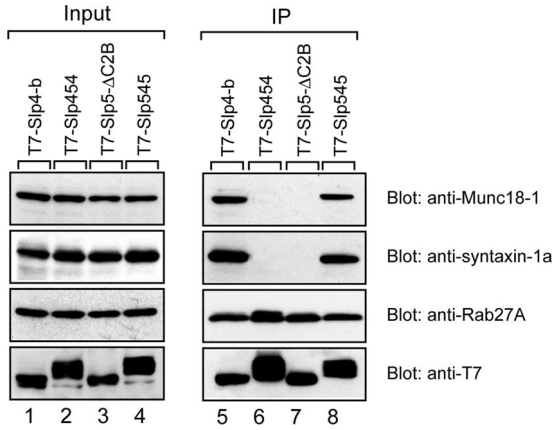

Figure 8. In vivo interaction between Slp4/5 chimeras and SNARE-related proteins in PC12 cells. Slp4-linker-domain–containing molecules (i.e., Slp4-b and Slp545; see lanes 5 and 8), but not Slp5-linker-domain–containing molecules (i.e., Slp454 and Slp5-ΔC2B; see lanes 6 and 7), efficiently immunoprecipitated Munc18-1 and syntaxin-1a. Immunoprecipitation (IP) and immunoblotting were performed as described in *Materials and Methods.* Input means one tenth the volume of the reaction mixtures used for immunoprecipitation (lanes 1–4).

Torii *et al.*, 2002, who showed that syntaxin-1a interacts with the N-terminal SHD in a Rab27A-dependent manner).

To confirm the above findings in PC12 cells, we further tested the interaction between the linker-domain–swapping mutants (i.e., Slp454 and Slp545) and endogenous Munc18-1, syntaxin-1a, or Rab27A by coimmunoprecipitation assay in PC12 cells. As anticipated, the Slp545 mutant interacted with endogenous Munc18-1, syntaxin-1a, and Rab27A, the same as Slp4-b did (lanes 5 and 8 in Figure 8), whereas Slp5-ΔC2B and Slp454 interacted with Rab27A alone, and not with Munc18-1 or syntaxin-1a (lanes 6 and 7).

Finally, we investigated the intracellular distribution of Slp4-a, Munc18-1, and syntaxin-1a in PC12 cells by immunofluorescence analysis. Comparison of the intracellular localization of NPY-Venus, mRFP-Slp4-a, and Munc18-1 in PC12 cells revealed that NPY-Venus labeled dense-core vesicles colocalized well with both mRFP-Slp4-a and Munc18-1 (Figure 9, A–D). Comparison of the intracellular localization of NPY-Venus, mRFP-Slp4-a, and syntaxin-1a (Figure 9, E–H) showed that colocalization between mRFP-Slp4-a (or NPY-Venus) and syntaxin-1a was very limited (i.e., colocalization was only observed immediately just beneath the plasma membrane; Figure 9H). These results, together with the results of the coimmunoprecipitation assay above, strongly suggest that Slp4-a interacts with Rab27A and Munc18-1 on dense-core vesicles and that the interaction between the Rab27A·Slp4-a·Munc18-1 complex and syntaxin-1a promotes anchoring of dense-core vesicles to the plasma membrane.

DISCUSSION

In the present study we demonstrated that five Slp isoforms tagged with mRFP are mainly targeted to dense-core vesicles in PC12 cells (Figure 1) and affect dense-core vesicle exocytosis differently (Figure 2). Expression of Slp4-a greatly increased the number of plasma membrane-docked inert vesicles and inhibited high-KCl–induced NPY-Venus release, whereas expression of either Slp3-a or Slp5, a Ca^{2+}-dependent-type Slp (Fukuda *et al.*, 2002; Fukuda, 2003), significantly enhanced high-KCl–induced NPY-Venus release without changing the number of vesicles docked to the plasma membrane. In addition, Slp4-a siRNA–expressing PC12 cells exhibited the docking defect, and high-KCl–induced NPY-Venus release events were significantly increased in them (Figure 6). The inhibitory effect of Slp4-a on dense-core vesicle exocytosis is perfectly correlated with its ability to interact with the Munc18-1·syntaxin-1a complex via the Slp4-a linker domain in PC12 cells, as revealed by TIRF microscopy combined with deletion and chimeric analyses (Figures 4, 5, 7, and 8). Because Slp4-a and Munc18-1 colocalized well on NPY-Venus–containing vesicles and the colocalization between Slp4-a and syntaxin-1a was limited to immediately adjacent to the plasma membrane (Figure 9), we propose the following model (Figure 10A, right panel): 1) Slp4-a is targeted to Rab27A on dense-core vesicles via the SHD; 2) Munc18-1 is then recruited and directly binds the linker domain of Slp4-a; and 3) Munc18-1 in the Slp4-a·Munc18-1 complex directly binds the closed conformation of syntaxin-1a in the plasma membrane. The resulting Rab27A·Slp4-a·Munc18-1·syntaxin-1a quadripartite complex links dense-core vesicles to the plasma membrane. Similar docking machinery consisting of Rab27A·Slp2-a·phosphatidylserine or Rab27A·rabphilin·SNAP-25 has recently been reported in melanosome anchoring to the plasma membrane in melanocytes (Kuroda and Fukuda, 2004) and docking of dense-core vesicles to the plasma membrane in PC12 cells (Tsuboi and Fukuda, 2005; Fukuda, 2006), respectively. Although this manuscript was being prepared, Slp4-a–deficient mice whose pancreatic β-cells contain decreased numbers of docked vesicles and exhibit in-

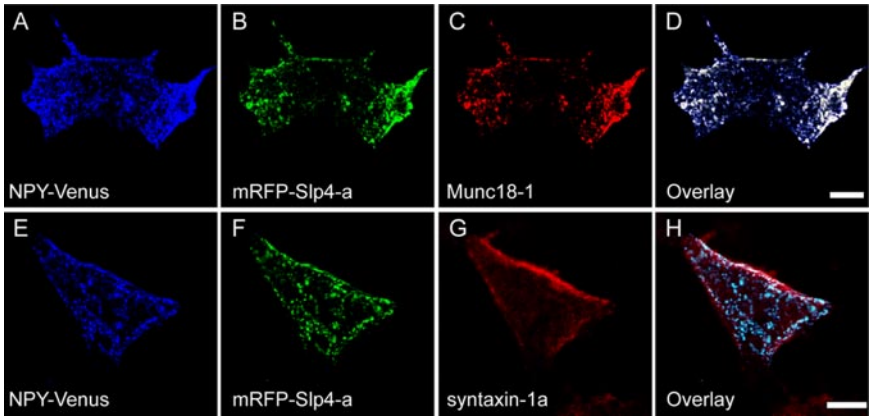

Figure 9. Colocalization of Slp4-a, Munc18-1, syntaxin-1a, and secretory peptide in PC12 cells. NPY-Venus (A and E) and mRFP-Slp4-a (B and F) were coexpressed in PC12 cells. Two days after transfection, the cells were fixed and stained with anti-Munc18-1 (C) or anti-syntaxin-1a antibody (G). The images of the cells were obtained by confocal microscopy. Scale bars, 10 μm. Note that Munc18-1 colocalized well with both the dense-core vesicle marker NPY-Venus and mRFP-Slp4-a (D), whereas syntaxin-1a partially colocalized with mRFP-Slp4-a (H) immediately adjacent to the plasma membrane.

creased insulin secretion activity have been reported (Gomi *et al.*, 2005), quite consistent with our own results. Although Gomi *et al.* (2005) claimed that direct interaction between Slp4-a and syntaxin-1a mediates vesicle docking to the plasma membrane (Figure 10A, left panel), our findings in this study strongly conflict with that notion and indicate that the interaction between the Slp4-a linker domain and the Munc18-1·syntaxin-1a complex mediates vesicle docking to the plasma membrane. Consistent with this, the level of expression of both Munc18-1 and syntaxin-1a was reduced in the Slp4-a–deficient mice (Gomi *et al.*, 2005).

Although Munc18-1–deficient mice are known to have normal synaptic structures (i.e., docking of synaptic vesicles to the presynaptic plasma membrane is normal; Verhage *et al.*, 2000), a defect in the dense-core vesicle docking to the plasma membrane in neuroendocrine cells has recently been reported (Voets *et al.*, 2001; Korteweg *et al.*, 2005). Moreover, Munc18-1 has been proposed to regulate more than one stage (e.g., docking and fusion) of dense-core vesicle exocytosis (Fisher *et al.*, 2001; Graham *et al.*, 2004; Ciufo *et al.*, 2005), possibly by binding different binding partners (e.g., syntaxin-1a and Doc2; Verhage *et al.*, 1997). How Munc18-1 controls the docking step of dense-core vesicle exocytosis, however, had never been elucidated. In the present study we demonstrated for the first time that Slp4-a is an in vivo Munc18-1–binding partner that contributes to the docking of dense-core vesicles to the plasma membrane of PC12 cells. This docking machinery seems to be specific to dense-core vesicles in certain neuroendocrine cells, because Slp4-a is not expressed in neurons (or on synaptic vesicles) and is unlikely to be involved in the synaptic vesicle-docking step.

Why do Slp4-a–deficient PC12 cells exhibit increased dense-core vesicle exocytosis? We think that the enhancement of dense-core vesicle exocytosis by Slp4-a knockdown might be explained by the presence of a variety of Rab3A and Rab27A effectors in neuroendocrine cells (Cheviet *et al.*, 2004; Fukuda,

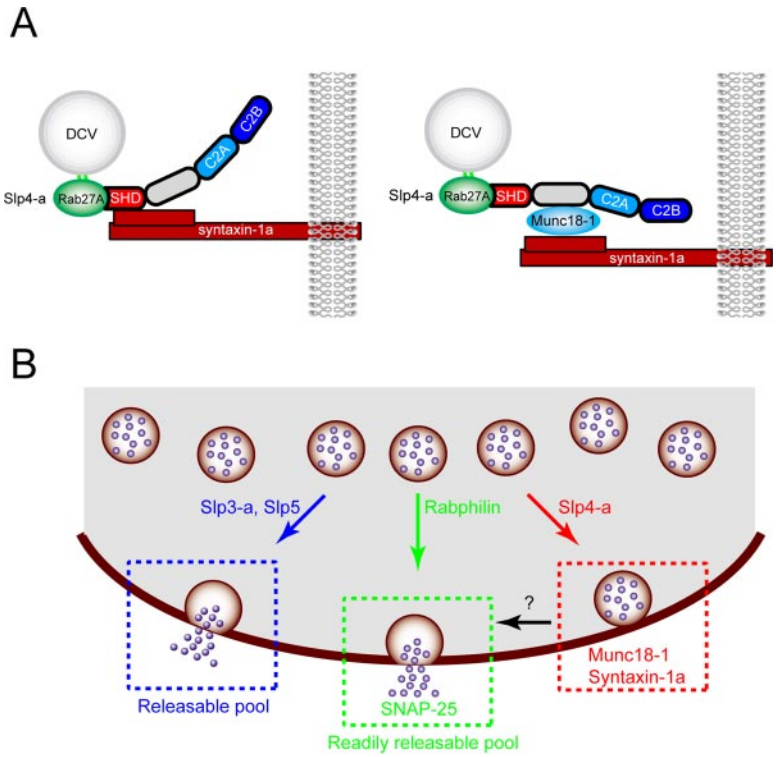

Figure 10. Proposed model for Slp/rabphilin-dependent dense-core vesicle exocytosis in neuroendocrine cells. (A) Vesicle docking machinery proposed by Gomi *et al.* (2005) (left panel) and by the authors based on the results of the present study (right panel). (B) Slp1~5 and rabphilin are recruited to dense-core vesicles through specific interaction with Rab27A/B on dense-core vesicles (Fukuda *et al.*, 2004 and this study). Rabphilin and Slp4-a promote docking of dense-core vesicles to the plasma membrane through interaction with SNAP-25 (Tsuboi and Fukuda, 2005; Fukuda, 2006) and Munc18-1·syntaxin-1a complex (shown in A, right panel), respectively. Dense-core vesicles docked to the plasma membrane by the former complex (i.e., Rab27·rabphilin·SNAP-25) undergo exocytosis in response to high-KCl stimulation (presumably corresponds to the "readily releasable pool"), whereas dense-core vesicles docked to the plasma membrane by the latter complex (i.e., Rab27·Slp4-a·Munc18-1·sytnaxin-1a) are insensitive to high-KCl stimulation. The physiological significance of the high-KCl-stimulation–insensitive population of vesicles (i.e., "inert vesicles") is currently unknown. Slp3-a and Slp5, Ca^{2+}-dependent-type Slps, promote sustained exocytosis of dense-core vesicles that are not predocked to the plasma membrane (presumably corresponds to the "releasable pool") by largely unknown mechanisms. In the absence of Slp4-a, other Ca^{2+}-dependent Slps or rabphilin presumably occupy Rab27 on the vesicles, and thereby promote sustained exocytotic events.

2005), and several Rab27A effectors (e.g., rabphilin, Slp4-a, Slp5, Noc2, and Slac2-c) are in fact expressed in PC12 cells or pancreatic β-cell lines (Fukuda *et al.*, 2002, 2004; Desnos *et al.*, 2003; Waselle *et al.*, 2003). For example, rabphilin has recently been shown to promote the docking of dense-core vesicles to the plasma membrane through simultaneous interaction with Rab27A on the dense-core vesicle and SNAP-25 at the plasma membrane via the C2B domain and enhance individual exocytotic events (Tsuboi and Fukuda, 2005). Thus, it is highly possible that other Rab27A effectors occupy Rab27A on dense-core vesicles, instead of Slp4-a, in Slp4-a–deficient cells and enhance dense-core vesicle exocytosis by promoting the recruitment, docking, and/or priming of dense-core vesicles (Figure 10B).

Regulated exocytosis is generally thought to occur at two different pools, a "readily releasable pool" and "releasable pool." In PC12 cells, the former pool corresponds to the initial high-KCl–induced NPY-Venus release by vesicles predocked to the plasma membrane, and the latter mainly corresponds to the sustained NPY-Venus release by newly recruited undocked vesicles. It is interesting that expression of Slp3-a or Slp5 in PC12 cells significantly increased the sustained NPY-Venus release (Figure 3C), suggesting that predocking of dense-core vesicles to the plasma membrane may not be required for dense-core vesicle exocytosis from the releasable pool. In addition, recent studies have demonstrated that mobile undocked vesicles support exocytosis more efficiently than immobile docked vesicles in the growth cones of PC12 cells, pancreatic β-cells, and hippocampal neurons (Han *et al.*, 1999; Tsuboi and Rutter, 2003; Tsuboi *et al.*, 2003; Silverman *et al.*, 2005). We therefore speculate that Slp3-a and Slp5 regulate the number of "release-competent" secretory vesicles or function as a priming factor together with an unidentified binding protein(s). Further study is needed to identify the binding proteins of Slp3-a and Slp5 and how Slp3-a and Slp5 facilitate dense-core vesicle exocytosis by PC12 cells or other types of secretory vesicle exocytosis (e.g., exocrine exocytosis and secretion by immune cells) at the molecular level.

In summary, we have demonstrated by in vivo binding assays and live cell TIRF imaging that Slp4-a interacts with syntaxin-1a in a Munc18-1–dependent manner via the linker domain of Slp4-a, and we propose that the Rab27A·Slp4-a·Munc18-1·syntaxin-1a complex mediates dense-core vesicle docking to the plasma membrane in PC12 cells.

ACKNOWLEDGMENTS

We thank Dr. Atsushi Miyawaki (Riken Brain Science Institute, Saitama, Japan) for kindly donating NPY-Venus and Eiko Kanno and Megumi Satoh for technical assistance. This work was supported in part by the Ministry of Education, Culture, Sports, and Technology of Japan (Grants 15689006, 16044248, 17024065, and 17657067 to M.F.), by the Kato Memorial Bioscience Foundation (M.F.), by The Sumitomo Foundation (M.F.), by the Mochida Memorial Foundation for Medical and Pharmaceutical Research (T.T.), by the Uehara Memorial Foundation (T.T.), and by the FY2005 DRI Research Grant (T.T.). T.T. was supported by Special Postdoctoral Researchers Program in Riken.

REFERENCES

An, S. J., and Almers, W. (2004). Tracking SNARE complex formation in live endocrine cells. Science *306,* 1042–1046.

Axelrod, D. (1981). Cell-substrate contacts illuminated by total internal reflection fluorescence. J. Cell Biol. *89,* 141–145.

Campbell, R. E., Tour, O., Palmer, A. E., Steinbach, P. A., Baird, G. S., Zacharias, D. A., and Tsien, R. Y. (2002). A monomeric red fluorescent protein. Proc. Natl. Acad. Sci. USA *99,* 7877–7882.

Cheviet, S., Waselle, L., and Regazzi, R. (2004). Noc-king out exocrine and endocrine secretion. Trends Cell Biol. *14,* 525–528.

Ciufo, L. F., Barclay, J. W., Burgoyne, R. D., and Morgan, A. (2005). Munc18-1 regulates early and late stages of exocytosis via syntaxin-independent protein interactions. Mol. Biol. Cell *16,* 470–482.

Coppola, T., Frantz, C., Perret-Menoud, V., Gattesco, S., Hirling, H., and Regazzi, R. (2002). Pancreatic β-cell protein granuphilin binds Rab3 and Munc-18 and controls exocytosis. Mol. Biol. Cell *13,* 1906–1915.

Desnos, C. *et al.* (2003). Rab27A and its effector MyRIP link secretory granules to F-actin and control their motion towards release sites. J. Cell Biol. *163,* 559–570.

Fisher, R. J., Pevsner, J., and Burgoyne, R. D. (2001). Control of fusion pore dynamics during exocytosis by Munc18. Science *291,* 875–878.

Fukuda, M. (2002). The C2A domain of synaptotagmin-like protein 3 (Slp3) is an atypical calcium-dependent phospholipid-binding machine: comparison with the C2A domain of synaptotagmin I. Biochem. J. *366,* 681–687.

Fukuda, M. (2003). Slp4-a/granuphilin-a inhibits dense-core vesicle exocytosis through interaction with the GDP-bound form of Rab27A in PC12 cells. J. Biol. Chem. *278,* 15390–15396.

Fukuda, M. (2004). RNA interference-mediated silencing of synaptotagmin IX, but not synaptotagmin I, inhibits dense-core vesicle exocytosis in PC12 cells. Biochem. J. *380,* 875–879.

Fukuda, M. (2005). Versatile role of Rab27 in membrane trafficking: focus on the Rab27 effector families. J. Biochem. (Tokyo) *137,* 9–16.

Fukuda, M. (2006). The role of synaptotagmin and synaptotagmin-like protein (Slp) in regulated exocytosis. Mol. Mech. Exocytosis (Regazzi, R., ed.), (*in press*) (http://eurekah.com/abstract.php?chapid=2872&bookid=218&catid=15).

Fukuda, M., Aruga, J., Niinobe, M., Aimoto, S., and Mikoshiba, K. (1994). Inositol-1,3,4,5-tetrakisphosphate binding to C2B domain of IP4BP/synaptotagmin II. J. Biol. Chem. *269,* 29206–29211.

Fukuda, M., Imai, A., Nashida, T., and Shimomura, H. (2005). Slp4-a/granuphilin-a interacts with syntaxin-2/3 in a Munc18–2-dependent manner. J. Biol. Chem. *280,* 39175–39184.

Fukuda, M., and Kanno, E. (2005). Analysis of the role of Rab27 effector Slp4-a/granuphilin-a in dense-core vesicle exocytosis. Methods Enzymol. *403,* 445–457.

Fukuda, M., Kanno, E., Saegusa, C., Ogata, Y., and Kuroda, T. S. (2002). Slp4-a/granuphilin-a regulates dense-core vesicle exocytosis in PC12 cells. J. Biol. Chem. *277,* 39673–39678.

Fukuda, M., Kanno, E., and Mikoshiba, K. (1999). Conserved N-terminal cysteine motif is essential for homo- and heterodimer formation of synaptotagmins III, V, VI, and X. J. Biol. Chem. *274,* 31421–31427.

Fukuda, M., Kanno, E., and Yamamoto, A. (2004). Rabphilin and Noc2 are recruited to dense-core vesicles through specific interaction with Rab27A in PC12 cells. J. Biol. Chem. *279,* 13065–13075.

Fukuda, M., Kojima, T., Aruga, J., Niinobe, M., and Mikoshiba, K. (1995). Functional diversity of C2 domains of synaptotagmin family: mutational analysis of inositol high polyphosphate binding domain. J. Biol. Chem. *270,* 26523–26527.

Fukuda, M., and Mikoshiba, K. (2001). Synaptotagmin-like protein 1–3: a novel family of C-terminal-type tandem C2 proteins. Biochem. Biophys. Res. Commun. *281,* 1226–1233.

Fukuda, M., Saegusa, C., and Mikoshiba, K. (2001). Novel splicing isoforms of synaptotagmin-like proteins 2 and 3: identification of the Slp homology domain. Biochem. Biophys. Res. Commun. *283,* 513–519.

Gomi, H., Mizutani, S., Kasai, K., Itohara, S., and Izumi, T. (2005). Granuphilin molecularly docks insulin granules to the fusion machinery. J. Cell Biol. *171,* 99–109.

Graham, M. E., Barclay, J. W., and Burgoyne, R. D. (2004). Syntaxin/Munc18 interactions in the late events during vesicle fusion and release in exocytosis. J. Biol. Chem. *279,* 32751–32760.

Han, W., Ng, Y. K., Axelrod, D., and Levitan, E. S. (1999). Neuropeptide release by efficient recruitment of diffusing cytoplasmic secretory vesicles. Proc. Natl. Acad. Sci. USA *96,* 14577–14582.

Imai, A., Yoshie, S., Nashida, T., Shimomura, H., and Fukuda, M. (2004). The small GTPase Rab27B regulates amylase release from rat parotid acinar cells. J. Cell Sci. *117,* 1945–1953.

Jahn, R., and Südhof, T. C. (1999). Membrane fusion and exocytosis. Annu. Rev. Biochem. *68,* 863–911.

Korteweg, N., Maia, A. S., Thompson, B., Roubos, E. W., Burbach, J. P., and Verhage, M. (2005). The role of Munc18-1 in docking and exocytosis of peptide hormone vesicles in the anterior pituitary. Biol. Cell *97,* 445–455.

Kuroda, T. S., and Fukuda, M. (2004). Rab27A-binding protein Slp2-a is required for peripheral melanosome distribution and elongated cell shape in melanocytes. Nat. Cell Biol. *6,* 1195–1203.

Kuroda, T. S., Fukuda, M., Ariga, H., and Mikoshiba, K. (2002a). The Slp homology domain of synaptotagmin-like proteins 1–4 and Slac2 functions as a novel Rab27A binding domain. J. Biol. Chem. *277,* 9212–9218.

Kuroda, T. S., Fukuda, M., Ariga, H., and Mikoshiba, K. (2002b). Synaptotagmin-like protein 5: a novel Rab27A effector with C-terminal tandem C2 domains. Biochem. Biophys. Res. Commun. *293,* 899–906.

Lang, T., Wacker, I., Steyer, J., Kaether, C., Wunderlich, I., Soldati, T., Gerdes, H. H., and Almers, W. (1997). Ca^{2+}-triggered peptide secretion in single cells imaged with green fluorescent protein and evanescent-wave microscopy. Neuron *18,* 857–863.

McAdara Berkowitz, J. K., Catz, S. D., Johnson, J. L., Ruedi, J. M., Thon, V., and Babior, B. M. (2001). JFC1, a novel tandem C2 domain-containing protein associated with the leukocyte NADPH oxidase. J. Biol. Chem. *276,* 18855–18862.

Mizushima, S., and Nagata, S. (1990). pEF-BOS, a powerful mammalian expression vector. Nucleic Acids Res. *18,* 5322.

Nagai, T., Ibata, K., Park, E. S., Kubota, M., Mikoshiba, K., and Miyawaki, A. (2002). A variant of yellow fluorescent protein with fast and efficient maturation for cell-biological applications. Nat. Biotechnol. *20,* 87–90.

Rizo, J., and Südhof, T. C. (2002). SNAREs and Munc18 in synaptic vesicle fusion. Nat. Rev. Neurosci. *3,* 641–653.

Rothman, J. E. (1994). Mechanisms of intracellular protein transport. Nature *372,* 55–63.

Segev, N. (2001). Ypt and Rab GTPases: insight into functions through novel interactions. Curr. Opin. Cell Biol. *13,* 500–511.

Silverman, M. A., Johnson, S., Gurkins, D., Farmer, M., Lochner, J. E., Rosa, P., and Scalettar, B. A. (2005). Mechanisms of transport and exocytosis of dense-core granules containing tissue plasminogen activator in developing hippocampal neurons. J. Neurosci. *25,* 3095–3106.

Strom, M., Hume, A. N., Tarafder, A. K., Barkagianni, E., and Seabra, M. C. (2002). A family of Rab27-binding proteins: melanophilin links Rab27a and myosin Va function in melanosome transport. J. Biol. Chem. *277,* 25423–25430.

Toonen, R. F., and Verhage, M. (2003). Vesicle trafficking: pleasure and pain from SM genes. Trends Cell Biol. *13,* 177–186.

Torii, S., Takeuchi, T., Nagamatsu, S., and Izumi, T. (2004). Rab27 effector granuphilin promotes the plasma membrane targeting of insulin granules via interaction with syntaxin 1a. J. Biol. Chem. *279,* 22532–22538.

Torii, S., Zhao, S., Yi, Z., Takeuchi, T., and Izumi, T. (2002). Granuphilin modulates the exocytosis of secretory granules through interaction with syntaxin 1a. Mol. Cell. Biol. *22,* 5518–5526.

Tsuboi, T., da Silva-Xavier, G., Leclerc, I., and Rutter, G. A. (2003). 5′-AMP-activated protein kinase controls insulin-containing secretory vesicle dynamics. J. Biol. Chem. *278,* 52042–52051.

Tsuboi, T., and Fukuda, M. (2005). The C2B domain of rabphilin directly interacts with SNAP-25 and regulates the docking step of dense-core vesicle exocytosis in PC12 cells. J. Biol. Chem. *280,* 39253–39259.

Tsuboi, T., McMahon, H. T., and Rutter, G. A. (2004). Mechanisms of dense core vesicle recapture following "kiss and run" ("cavicapture") exocytosis in insulin-secreting cells. J. Biol. Chem. *279,* 47115–47124.

Tsuboi, T., Ravier, M. A., Xie, H., Ewart, M. A., Gould, G. W., Baldwin, S. A., and Rutter, G. A. (2005). Mammalian exocyst complex is required for the docking step of insulin vesicle exocytosis. J. Biol. Chem. *280,* 25565–25570.

Tsuboi, T., and Rutter, G. A. (2003). Multiple forms of "kiss-and-run" exocytosis revealed by evanescent wave microscopy. Curr. Biol. *13,* 563–567.

Tsuboi, T., Zhao, C., Terakawa, S., and Rutter, G. A. (2000). Simultaneous evanescent wave imaging of insulin vesicle membrane and cargo during a single exocytotic event. Curr. Biol. *10,* 1307–1310.

Verhage, M., de Vries, K. J., Roshol, H., Burbach, J. P., Gispen, W. H., and Südhof, T. C. (1997). DOC2 proteins in rat brain: complementary distribution and proposed function as vesicular adapter proteins in early stages of secretion. Neuron *18,* 453–461.

Verhage, M. *et al.* (2000). Synaptic assembly of the brain in the absence of neurotransmitter secretion. Science *287,* 864–869.

Voets, T., Toonen, R. F., Brian, E. C., de Wit, H., Moser, T., Rettig, J., Südhof, T. C., Neher, E., and Verhage, M. (2001). Munc18-1 promotes large dense-core vesicle docking. Neuron *31,* 581–591.

Wang, J., Takeuchi, T., Yokota, H., and Izumi, T. (1999). Novel rabphilin-3-like protein associates with insulin-containing granules in pancreatic beta cells. J. Biol. Chem. *274,* 28542–28548.

Waselle, L., Coppola, T., Fukuda, M., Iezzi, M., El Amraoui, A., Petit, C., and Regazzi, R. (2003). Involvement of the Rab27 binding protein Slac2c/MyRIP in insulin exocytosis. Mol. Biol. Cell *14,* 4103–4113.

Yi, Z., Yokota, H., Torii, S., Aoki, T., Hosaka, M., Zhao, S., Takata, K., Takeuchi, T., and Izumi, T. (2002). The Rab27a/granuphilin complex regulates the exocytosis of insulin-containing dense-core granules. Mol. Cell. Biol. *22,* 1858–1867.

Zerial, M., and McBride, H. (2001). Rab proteins as membrane organizers. Nat. Rev. Mol. Cell Biol. *2,* 107–117.

Zhao, S., Torii, S., Yokota-Hashimoto, H., Takeuchi, T., and Izumi, T. (2002). Involvement of Rab27b in the regulated secretion of pituitary hormones. Endocrinology *143,* 1817–1824.